Phase Coded Waveforms with Optimal Peak-to-Sidelobe Ratio and Optimal Confined Bandwidth

Yunhan Dong
National Security and ISR Division
Defence Science and Technology Group
Australia
yunhan.dong@dst.defence.gov.au

Abstract— **Among phase continuously and randomly coded waveforms it is shown that the quadriphase-coded (QPC) waveform has the best peak-to-sidelobe ratio (PSR). Hence a QPC waveform coded by a binary sequence with the minimum peak sidelobe level (PSL) results in a continuous phase modulated (CPM) waveform with the optimal PSR. To improve the spectrum of the original QPC waveform, the Gaussian minimum shift keying (GMSK) coding function is used to code the QPC waveform making the phase continuous and differentiable. In addition, a spectral optimisation model is proposed to further refine the GMSK-coded QPC waveform. The final product is a constrained-bandwidth constant-amplitude waveform whose phase profile is continuous, smooth and differentiable. It has optimal PSR and optimal spectrum which quite satisfies the criteria specified by the US National Telecommunications and Information Administration (NTIA).**

Keywords—Phase-coded waveform; Peak-to-sidelobe ratio; waveform design

I. INTRODUCTION

As technologies especially digital signal processing (DSP) advance, there is a potential demand for radar replacing (at least for some modes) its traditional recurrent linear or nonlinear frequency modulated (LFM or NLFM) waveforms by non-recurrent non-predictable phase randomly coded waveforms. To generate deployable good phase randomly coded waveforms which have constant amplitude and constrained-bandwidth is a challenge. Since for constant-amplitude waveforms, the phase change rate, i.e. the derivative of the phase with respect to time, stands for the instantaneous angular frequency (i.e. $2\pi f(t) = d\varphi(t)/dt$), high phase change rates mean the presence of high frequency components in its spectrum. Therefore, it naturally requires that the phase profile of the waveform be continuous, smooth and differentiable. On the other hand, waveforms need to have good pulse compression ratios to effectively utilise the valuable spectrum and provide coherent processing gains. The waveforms also need to provide good peak-to-sidelobe ratio (PSR) to mitigate possible masking effects of clutter and strong targets on small targets. It also requires that the waveforms have a good Doppler tolerance as well as other features to satisfy radar's requirements.

The phase of the phase-coded waveforms can be divided into two categories: continuous phase modulated (CPM) and discontinuous phase modulated (DPM). Examples of DPM waveforms include biphase-coded and polyphase coded waveforms [1; Chapter 20, 2; Chapter 2]. DPM waveforms, if coded appropriately, can provide best PSR (i.e. the lowest sidelobe levels). For instance, Nunn and Coxton [3] have reported the identified polyphase Barker codes of length 64-70, 72, 76, and 77. The polyphase Barker codes 77 shall give PSR of $20\log_{10}(77/1) = 37.7$ dB. Unfortunately, DPM waveforms have a very slow spectral roll-off pattern outside the specified bandwidth. According to the time-frequency uncertainty principle [4; page 27], the spectrum of a DPM waveform spans widely (theoretically from minus infinity to plus infinity) and the roll-off of its spectral sidebands is slow. This raises issues in its implementation. The requirement of a wider bandwidth not only increases the complexity of the hardware but also reduces the SNR as a receiver with a wider bandwidth is required. It also wastes the valuable spectral bandwidth. In addition, sidebands of the spectrum are a source of electromagnetic interference (EMI), and have the potential interference with other RF systems operating nearby.

On the other hand, the CPM waveforms receive great interest in radar community [5, 6]. Because of its continuous phase, the roll-off of spectral sidebands is in a much faster fashion. For instance, the peak spectral sidelobe of the QPC waveform (the QPC is a special form of CPM waveforms) is approximately -23 dB with the following sidelobes falling off at 12 dB per octave. By comparison, the peak spectral sidelobe of the biphase-coded waveform is only approximately -13 dB with the following sidelobes falling off at 6 dB per octave [2; Chapter 2, 7].

The amplitude of the phase-coded waveforms can also be divided into two categories: constant-amplitude and fluctuating –amplitude. Since most radar transmitter power amplifiers are operated in a saturated mode, the constant-amplitude waveforms are preferred. If fluctuating-amplitude waveforms have to be used (due to the spectral or other requirement), architectures such as the linear amplification with nonlinear component (LINC) may have to be applied in radar design to avoid operating the transmitter high-power amplifiers in the linear mode [8]. In the LINC architecture, the amplitude fluctuated waveform is decomposed into two constant amplitude components that normally requires two identical amplifiers to implement.

All published constant amplitude phase-coded waveforms with continuous or discontinuous phase have a problem that

they fail to satisfy the spectral criteria (more details later). To overcome, Jakabosky *et al.* [8, 9] proposed a compromised design to allow the amplitude fluctuating a bit to satisfy the spectral requirement and use the LINC implementation.

The goal of this paper is to obtain CPM waveforms that have constant amplitude, continuous and differentiable phase, optimal PSR (with respect to the CPM category) and optimal spectral distribution (i.e. the unwanted spectral sidebands are suppressed to the minimum) to satisfy the spectral requirement.

II. Optimal PSR Waveforms with Continuous and Differentiable Phase

A. *Continous Phase*

To code a phase-coded waveform, a pulse T is normally equally divided into N chips (intervals), and the duration of each chip is τ_c (N is also the pulse compression ratio if N chips are coded independently). The phase profile of a CPM waveform can be expressed as [5],

$$\varphi(t)=\begin{cases}\varphi_{n-1}=\sum_{k=0}^{n-1}\Delta\varphi_k & t=(n-1)\tau_c \\ \varphi_{n-1}+\Delta\varphi_n\int_0^{t-(n-1)\tau_c} g(\xi)d\xi & (n-1)\tau_c\le t\le n\tau_c\end{cases} \quad (1)$$

where $\Delta\varphi_n$ is the phase change for the n^{th} chip, $n=1,\cdots,N$; $\Delta\varphi_0$ is the initial phase of the waveform. Unless necessary, we let $\Delta\varphi_0=0$. The function $g(t)=d\varphi(t)/dt/\Delta\varphi_n$ is the normalised derivative of the phase function, i.e. the instantaneous frequency response function. Obviously, if $g(t)$ is continuous, $\varphi(t)$ is also continuous. Typical frequency response functions $g(t)$ include rectangular window, raised cosine and GMSK as well as few others [10, 11; Chapter 2]. Table 1 provides the math expressions for the three popular functions.

Table 1: Math expressions for three typical frequency response functions $g(t)$.

Name	Math expression
Rectan-gular	$g(t)=\begin{cases}1/\tau_c & 0\le t\le\tau_c\\ 0 & \text{elsewhere}\end{cases}$
Raised Cosine	$g(t)=\begin{cases}[1-\cos(2\pi(t+\Delta\tau)/(\tau_c+2\Delta\tau))]/(\tau_c+2\Delta\tau) & -\Delta\tau\le t\le\tau_c+\Delta\tau\\ 0 & \text{elsewhere}\end{cases}$
GMSK	$g(t)=\begin{cases}\beta\left[erf\left(\pi B_b\tau_c\sqrt{\frac{2}{\ln 2}}\left(\frac{t-\Delta\tau}{\tau_c}+0.5\right)\right)\right. \\ \left.-erf\left(\pi B_b\tau_c\sqrt{\frac{2}{\ln 2}}\left(\frac{t-\Delta\tau}{\tau_c}-0.5\right)\right)\right] & -\Delta\tau\le t\le\tau_c+\Delta\tau\\ 0 & \text{elsewhere}\end{cases}$

The $erf(\cdot)$ function in Table 1 is the error function, given by,

$$erf(t)=\frac{2}{\sqrt{\pi}}\int_0^t e^{-\tau^2}d\tau \quad (2)$$

If the rectangular window is used in (1), the coded phase within each chip has a linearly increase/decrease fashion. If one select a random phase $-\pi\le\Delta\varphi_n\le\pi$, the coded waveform is a polyphase-coded CPM waveform [5]. A random phase $\Delta\varphi_n$ drawn from a uniform distribution on $[-\pi,\pi]$ is equivalent to the product of a random binary number (1 or -1) times a random phase drawn from a uniform distribution on $[0,\pi]$. Therefore, a polyphase CPM waveform can be considered as a CPM waveform coded by a binary sequence and a random phase draw of $0\le\Delta\varphi_n\le\pi$. If the random phase draw is fixed at $\Delta\varphi_n=\pi/2$, the resulted waveform is a QPC waveform. The QPC waveform was first proposed by Taylor, Jr. and Blinchikoff [7], though the concept of CPM was not used, instead a half-cosine waveform was used as a base waveform to code the QPC waveform [7]. It can be shown that waveforms coded by **(1)** and the method proposed in [7] are identical.

We (and the readers) can verify that the for the same binary sequence, the QPC waveform (i.e. fixed phase draw of $\Delta\varphi_n=\pi/2$) has the best PSR than the polyphase CPM waveforms (i.e. random phase draw of $0\le\Delta\varphi_n\le\pi$). Figure 1 shows an example.

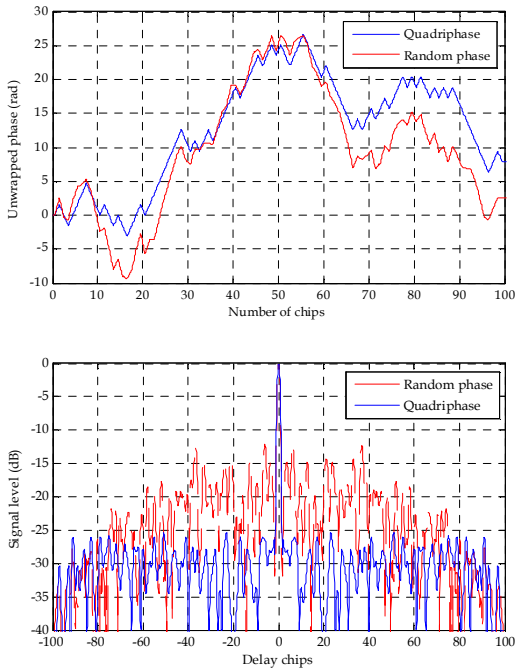

Figure 1: (top) QPC and polyphase phase profiles coded by an optimal PSL binary sequence with N = 100 and PSL = 5; (b) the corresponded autocorrelation profiles.

The spectra of the polyphase CPM and the QPC waveforms are shown in Figure 2. Statistically, two spectra are the same. However, the later has a much better PSR. The PSR of a QPC waveform is determined by the binary sequence. Therefore using the binary sequences that have the optimal peak sidelobe level (PSL) [12] will result in QPC waveforms that also have the optimal PSR among the CPM waveforms.

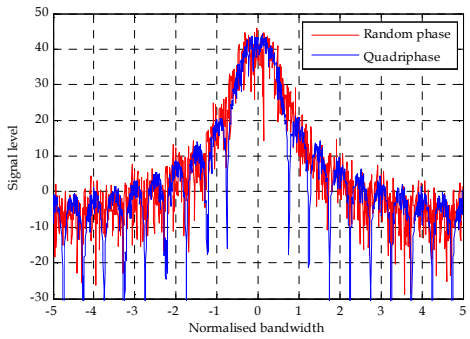

Figure 2: Spectra of the polyphase CPM and the QPC waveforms.

B. Continous and Differentiable Phase

The phase of QPC waveform is continuous but is not differentiable at the turning points. To have a better spectral distribution (i.e. lower spectral sidebands), it is preferable that the phase is not only continuous but also differentiable. To make the phase of QPC waveform differentiable, we can use the GMSK window function to code the phase. GMSK window is a Gaussian-shape window function [10] that has zeros slopes at the two ends making the phase of GMSK coded QPC waveform continuous and differentiable everywhere. This further improves its spectrum. Figure 3 compares the spectra of the original QPC and GMSK-coded QPC waveforms.

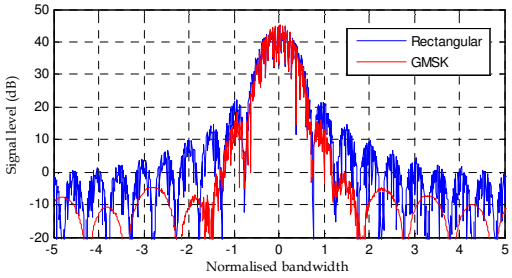

Figure 3: Comparison of the spectra of the original QPC and GMSK coded QPC waveforms ($N=100$).

III. SUPPRESSION OF SPECTRAL SIDEBANDS BY OPTIMISATION

The GMSK-coded QPC waveforms have improved their spectral distribution. However, according to the radar spectrum engineering criteria (RSEC) specified by the US National Telecommunications and Information Administration (NTIA), the undesired spectral sidebands need to be 40 dB below the peak of the spectral mainlobe and have a 20 dB/decade or 30 dB/decade roll-off rate [13; Chapter 5]. To satisfy these criteria, the spectral sidebands shown in Figure 3 need to be suppressed. To achieve this, a spectrum optimisation model is designed.

Let $s[t_n]$, $n=1,\cdots,M$ be the time samples of the waveform ($M=LN$, L is the number of samples per chip), $s[f_k]$, $k=-M/2,\cdots,0,\cdots,M/2$ be the associated spectral samples, and $y[t_n]$ be the amplitude of the associated aperiodic auto-correlation samples, $n=-(M-1),\cdots,0\cdots,(M-1)$. The spectrum optimization model is given by,

$$\begin{cases} \min\limits_{s[t]} \ \Sigma_{\cos t} = \sum\limits_{k=-M/2}^{M/2} w_k \left|s[f_k]\right|^2 + \sum\limits_{\substack{i=-M-1 \\ i\in \text{sidelobes}}}^{M-1} q_i \Delta y_i (\text{if } \Delta y_k > 0) \\ \text{subject to} \quad \left|s[t_n]\right|^2 = 1 \quad \forall \ n=1,\cdots,M \end{cases} \tag{3}$$

where $\{w_k\}$ and $\{q_i\}$ are appropriate weights to govern the optimisation process, $\Delta y_k = y[t_k] - y_0$ (y_0 is a constant determined by the PSR of the sequence) is the change of the sidelobe and only if the sidelobe increases, the penalty is applied.

Since the above model is nonconvex and highly nonlinear, the initial state is critical. The GMSK-coded QPC waveform is a good start, as the waveform has the constant-amplitude, continuous and differentiable phase. Note that in (3), the condition of continuous and differentiable phase is not explicitly included in the constraints. Since the confined bandwidth in the frequency domain has implicitly covered this constraint. In other words, if the spectrum is confined, the phase of the waveform must be continuous and differentiable. We also found that, for the GMSK-coded QPC waveform as the initial state, the PSR can maintain approximately unchanged, hence the penalty for possible increase in sidelobes can be removed to reduce the complexity of the optimisation model. The actual optimisation model used in this paper is,

$$\begin{cases} \min\limits_{s[t]} \quad \Sigma_{\cos t} = \sum\limits_{k=-M/2}^{M/2} w_k \left|s[f_k]\right|^2 \\ \text{subject to} \quad \left|s[t_n]\right|^2 = 1 \quad \forall \ n=1,\cdots,M \end{cases} \tag{4}$$

To optimise the spectrum, we selected $w_k = 0$ for the desired bandwidth, i.e. no penalty for spectral components within this bandwidth, and $w_k = 1$ for the spectral components outside the confined bandwidth. This is shown in Figure 4.

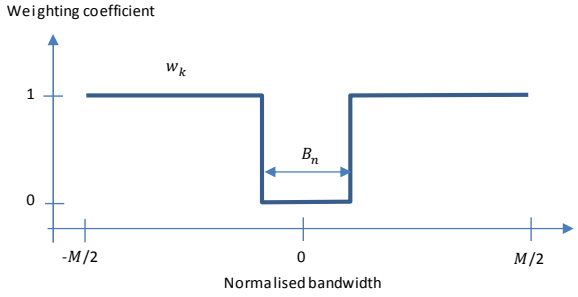

Figure 4: Weighting coefficients used in the optimisation model. B_n is the desired normalised bandwidth of the waveform. In general, the waveform is over-sampled for transmission $(M > B_n)$.

The optimisation model given by (4) is a nonlinear model. In our implementation the model was approximated to a linear model and the final waveform was obtained through the iterative process. The convergence of iteration is shown in Figure 5. Shown in the top plot is the total cost Σ_{cost} for the

waveform with constant-amplitude whereas the bottom plot shows the maximum amplitude error should the spectral bandwidth be truncated to the confined bandwidth. Although the convergence is slow, we can see both the cost and maximum amplitude error monotonically decrease. Finally when the amplitude error or cost is sufficiently small, we can terminate the process and assign the constant to the amplitude. The whole iteration on a desktop computer took a few seconds to tens of minutes depending on the number samples of the waveform.

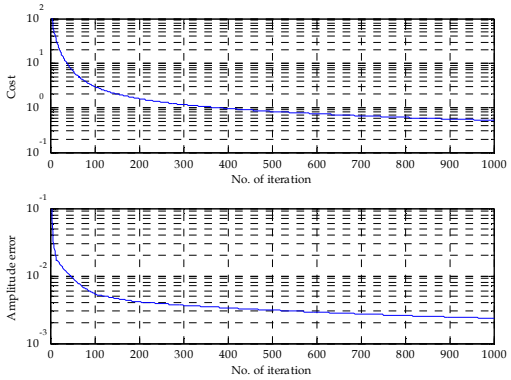

Figure 5: Both the cost and the maximum amplitude error monotonically decrease with iteration.

Figure 6 shows the phase profiles of the initial waveform (i.e. the GMSK-coded QPC waveform) and the final waveform (i.e. the spectrum optimised). It can be see the difference is very small. The final waveform still has the continuous and differentiable phase profile.

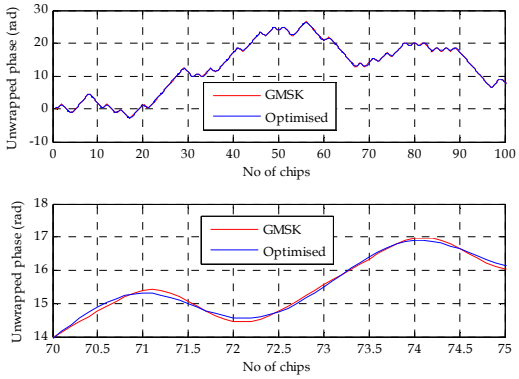

Figure 6: Two phase profiles of the initial GMSK-coded QPC waveform and the final optimised waveform. The bottom plot is a zoomed-in part of the top plot showing details of the profiles.

The spectra of the GMSK-coded and the optimised waveforms are shown in Figure 7. It can be seen that the optimised spectrum well satisfies the RSEC's criteria. The unwanted spectral sidebands have been greatly suppressed. The pulse compressed range profiles of the GMSK-coded QPC and the optimised waveforms are shown Figure 8. Essentially, and both profiles are identical.

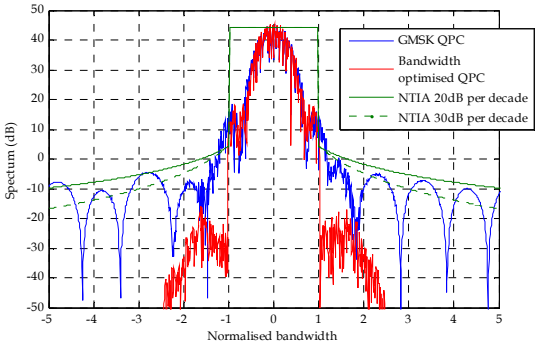

Figure 7: Comparison of the spectra of the GMSK-coded QPC waveform and the optimised waveform. The normalised bandwidth for the optimised waveform was specified from −1 to 1. The optimised spectrum are well within the RSEC's criteria.

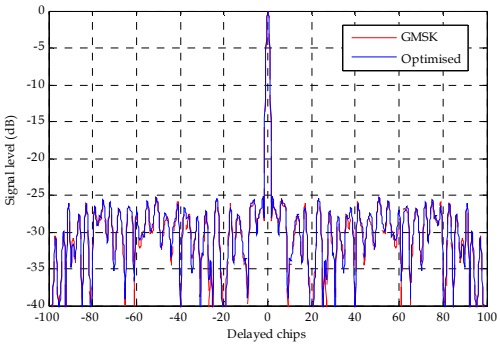

Figure 8: Pulse compressed range profiles of the original GMSK-coded QPC waveform and the optimised waveform.

To test the proposed model, we generated 1000 non-recurrent waveforms initially coded by the GMSK QPC algorithm. Each of the waveform consisted of 3240 chips and each chip was sampled by 5. The normalized bandwidth is specified by 2. If the waveform is sampled into a pulse of 10 and 20 μs, the bandwidth of the waveform would be 648 MHz and 324 MHz, respectively. The spectra of these 1000 waveforms are shown in Figure 9. It can be seen the spectral sidebands are approximately 60 dB below the peak of the mainlobe, much better than the 40 dB benchmark specified by the NTIA RSEC. The autocorrelation profile of one of the waveforms (all have statistically identical autocorrelation profiles) is shown in Figure 10, achieving 33 dB PSR.

I. CONCLUSIONS

None of the phase randomly coded waveforms published in the literature satisfies the spectral requirement. This paper proposes a nonlinear optimisation model implemented in a linear iteration process to confine the spectrum of the waveform. The initial waveform was coded using the GMSK-coded QPC waveform. The final waveform has constant amplitude, continuous and differentiable phase and more importantly, the confined bandwidth. If the binary sequence used to code the waveform has the minimum PSL, the resulted

waveform has not only the optimal PRS but also the lowest unwanted spectral sidebands.

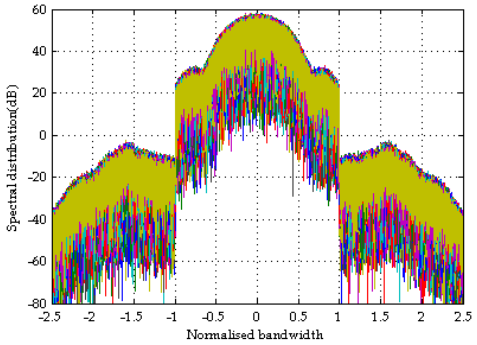

Figure 9: Spectra of 1000 waveforms. Each waveform consists of 3240 chips and each chip sampled by 5.

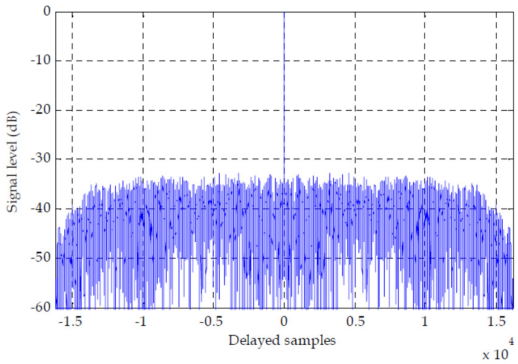

Figure 10: Autocorrelation profile of the optimised waveform composed of 3240 chips.

REFERENCES

[1] M. A. Richards, J. A. Scheer and W. A. Holm: "Principles of Modern Radar: Basic Principles", (Scitech Publishing Inc., 2010)

[2] W. L. Melvin and J. A. Scheer: "Principles of Modern Radar Vol. II: Advanced Techniques", (SciTech Publishing Inc., 2013)

[3] C. J. Nunn and G. E. Coxson: "Polyphase pulse compression codes with optimal peak and integrated sidelobes," *IEEE Trans on Aerospace and Electronic Systems*, 45, (2), 2009, pp. 775-781

[4] V. C. Chen and H. Ling: *Time-Frequency Transforms for Radar Imageing and Signal Analysis*, (Artech House, 2002)

[5] S. D. Blunt, M. Cook, J. Jakabosky, J. De Graaf and E. Perrins: "Polyphase-coded FM (PCFM) radar waveforms, Part I: Implementation," *IEEE Trans on Aerospace and Electronic Systems*, 50, (3), 2014, pp. 2218-2229

[6] S. D. Blunt, J. Jakabosky, M. Cook, S. Seguin and E. Mokole: "Polyphase-coded FM (PCFM) radar waveforms, Part II: Optimasation," *IEEE Trans on Aerospace and Electronic Systems*, 50, (3), 2014, pp. 2230-2241

[7] J. W. Taylor Jr. and H. J. Blinchikoff: "Quadriphase code - A radar pulse compression signal with unique characteristics," *IEEE Trans on Aerospace and Electronic Systems*, 24, (2), 1988, pp. 156-170

[8] J. Jakabosky, S. D. Blunt and T. Higgins: "Ultra-low sidelobe waveform design via spectral shaping and LINC transmit architecture", *IEEE Radar Conference (RadarCon)*, (2015)

[9] J. Jakabosky, S. D. Blunt and B. Himed: "Waveform design and receive processing nonrecurrent nonlinear FMCW radar", *IEEE Radar Conference (RadarCon)*, (2015)

[10] F. Adachi and K. Ohno: "Performance analysis of GMSK frequency detection with decision feedback equalisation in digital land mobile radio," *IEE Proceedings, Pt F*, 135, (3), 1988, pp. 199-207

[11] J. B. Anderson, T. Aulin and C. Sundburg: *Digital Phase Modulation*, (Plenum Press, 1986)

[12] C. J. Nunn and G. E. Coxson: "Best-known autocorrelation peak sidelobe levels for binary codes of length 71 to 105," *IEEE Trans on Aerospace and Electronic Systems*, 44, (1), 2008, pp. 392-395

[13] NTIA: *Manual of Regulations and Procedures for Federal Radio Frequency*, (National Telecommunications and Information Administration, 2015)